Journal of Orthopaedic Surgery and Research

RESEARCH

Open Access

Exosomal Manf originated from endothelium regulated osteoclast differentiation by down-regulating NF-κB signaling pathway

Zhilong Pi[1,2†], You Wu[2†], Xinyu Wang[2†], Pingyue Li[2*] and Renkai Wang[2*]

Abstract

Background Endothelium-derived exosomes has been reported to enhanced osteogenesis. However, the role of endothelial exosomes on osteoclastgenesis is still unknown.

Methods Human umbilical vein endothelial cells (HUVECs) were used to isolate exosomes. PBS or HUVEC-Exos were used to treat RAW 264.7 cells. Then, the preconditioned RAW 264.7 cells were subjected to TRAP staining and RT-qPCR assays. In vivo, we constracted osteoporosis mice model. PBS or HUVEC-Exos were injected through tail vein after ovariectomy surgery. Bone mass was assessed by micro-CT and TRAP staining. Furthermore, we conducted RNA sequencing and found the genes that were differentially expressed.

Results Osteoclast differentiation was inhibited by endothelium-derived exosomes in this study. Moreover, HUVEC-Exos demonstrated a specific action on bones to promote in vivo bone resorption. Furthermore, exosomal Manf promoted bone resorption via down-regulating NF-κB signaling, and HUVEC-Exos Manf inhibited osteoclast differentiation in vivo.

Conclusion HUVEC-exosomal Manf suppressed osteoclastogenesis via down-regulating NF-κB signaling.

Keywords Endothelium, Exosome, Osteoclast, NF-κB, Manf

Introduction

Low bone mass, the breakdown of the bone's microstructure, and increased bone fragility leading to fractures are the hallmarks of osteoporosis (OP), a disease that affects the entire bone [1]. Osteoporosis primarily affects older individuals and postmenopausal women [2, 3]. With the population aging, osteoporosis-induced fractures not only present challenges for patients and their families but also impose a significant burden on society and healthcare systems [4]. The processes of osteoblast-mediated bone production and osteoclast-mediated bone resorption are in a state of dynamic balance [5]. However, excessive osteoclast activation can cause bone loss, which in turn causes osteoporosis. Originating from the haematopoietic lineage of monocytes or macrophages, osteoclasts possess the ability to adhere to the bone matrix and break down it by secreting lytic enzymes and acids [6]. Thus, inhibition of osteoblast differentiation can delay bone loss caused by osteoporosis.

Extracellular vesicles range from 30 to 200 nm in diameter and are known as exosomes [7]. They comprise a plethora of active constituents, including proteins,

†Zhilong Pi, You Wu and Xinyu Wang are contributed equally to this work.

*Correspondence:
Pingyue Li
lipingyue@smu.edu.cn
Renkai Wang
501214241@qq.com
[1] Guangzhou University of Chinese Medicine, No. 132, Outer Ring East road, Guangzhou 510010, Guangdong, China
[2] Guangdong Key Lab of Orthopaedic Technology and Implant Materials, Key Laboratory of Trauma and Tissue Repair of Tropical Area of PLA, Hospital of Orthopaedics, General Hospital of Southern Theater Command of PLA, 111 Liuhua Road, Guangzhou, Guangdong, China

nucleic acids, and growth factors, which facilitate intercellular communication [8]. Additionally, exosomes are highly stable and exhibit low immunogenicity [9–11]. These characteristics render exosomes a promising therapeutic modality for various diseases [12–14]. Furthermore, Extracellular vesicles can be potential cell therapy for COVID-19 management and regenerative medicine [15, 16]. Vascular endothelial cell-derived exosomes have been shown to target bone and block osteoclast activity, which delays the onset of osteoporosis [17–19]. However, the mechanism of osteoclast differentiation by umbilical vein vascular endothelial stem cells remains unclear.

Thus, it was demonstrated that HUVEC-Exos played an important role in osteoclast differentiation. Furthermore, HUVEC-Exos were found to inhibited osteoclastgenesis in vitro and in vivo. Therefore, the present investigation primarily focused on the impact of HUVEC-Exos on bone resorption.

Methods and materials

Cell culture

HUVECs were obtained from Cyagen Biotechnology (USA) and were subjected to culturing Dulbecco's Modified Eagle's Medium (DMEM high glucose, Sigma, USA) rich in glucose. In the medium, penicillin–streptomycin (1%, Gibco, USA) and bovine serum (10%, FBS; VivaCell, Shanghai, China) were added to form a complete medium. RAW 264.7 cells were acquired from the American Type Culture Collection (USA), which were then cultured in a complete DMEM medium. Both cell lines were cultivated at 37 °C with 5% CO_2.

Exosome isolation

Exosome isolation and characterization were performed following the previously reported method [10]. Briefly, HUVEC cells were cultivated in complete media with EV-free FBS (SBI) for over 24 h. The supernatant containing HUVEC-Exos was subjected to centrifugation at 3,000 rpm for 40 min, followed by 20,000 rpm for 60 min. The supernatant was filtered out and subsequently centrifuged at 120,000×g for 70 min and rinsed with PBS. Finally, suspended HUVEC-Exos in PBS were kept at −4 °C for future use.

Exosome identification

The properties of HUVEC-Exos, including shape, particle size, and markers, were determined by utilizing transmission electron microscopy (TEM), western blotting (WB), and nanoparticle tracking analysis (NTA), which were performed as previously described [10].

Western blot experiment

The Beyotime protein extraction kit was employed to extract the total proteins from the collected cells. The equal volume of protein samples was loaded, separated using SDS-PAGE, and then moved onto polyvinylidene difluoride (PVDF) membranes measuring 0.22-μm in diameter. The membranes underwent an overnight treatment with specific antibodies after being blocked with 5% skim milk. The primary antibodies employed were GAPDH (1:1000), HSP70 (1:1000), CD9 (1:1000), and CD63 (1:1000), all sourced from Abcam. After that, the membranes were exposed to secondary antibodies labeled with horseradish peroxidase (HRP) for an hour at the ambient temperature.

Osteoclast differentiation in vitro

In a 96-well plate, the RAW 264.7 cells were cultivated (1×10^5 cells/well) to stimulate osteoclast differentiation. Following this, the cultured cells in complete DMEM media were supplemented with 30 ng/mL M-CSF (PeproTech) and 100 ng/mL soluble RANKL (PeproTech) for 7 days, with the medium being changed every 2 days. On Day 7, TRAP staining was conducted via a commercial kit (Sigma). Quantitive positive TRAP staining cells analysis was used by ImageJ software.

Real-time PCR

The extractraction of total RNA from cells was carried out after their harvesting and treatment with Trizol reagent. The concentration of RNA was determined while employing a Thermo Fisher Scientific NanoDrop-2000 spectrophotometer. Subsequently, a stem-loop reverse transcriptase primer kit (Ribobio, Guangzhou, China) was used to reverse-transcribe miRNA samples. SYBR Prime Script kit (Takara Bio Inc., Shiga, Japan) was used to conduct a triplicate quantitative reverse transcription polymerase chain reaction (qRT-PCR). The relative expression variation was determined using the comparative Ct ($2^{-\Delta\Delta Ct}$) method. The primers used for real-time PCR are listed in Table 1.

Animals

The General Hospital of the Southern Theatre Command of the PLA, located in Guangzhou, China, provided the female C57BL/6 mice. Within the animal center's specific pathogen-free (SPF) facilities, each mouse was kept. The Experimental Animal Centre of the General Hospital of the Southern Theatre Command of the PLA, Guangzhou, China, approved all animal care procedures and tests performed in this study. We constructed the osteoporosis (OP) model by bilateral removal of mice ovaries after adaptive feeding

Table 1 Primers list

Gene name		Sequence 5′–3′	Length	Tm	Accession
Gapdh	Forward primer 5′–3′	AAT GGA TTT GGA CGC ATT GGT	21	60.6	PrimerBank ID 6679938c1
	Reverse primer 5′–3′	TTT GCA CTG GTA CGT GTT GAT	21	60.2	
Ctsk	Forward primer 5′–3′	CTC GGC GTT TAA TTT GGG AGA	21	60.4	PrimerBank ID 142352209c1
	Reverse primer 5′–3′	TCG AGA GGG AGG TAT TCT GAG T	22	61.2	
Nfatc1	Forward primer 5′–3′	GGA GAG TCC GAG AAT CGA GAT	21	60.2	PrimerBank ID 255759924c1
	Reverse primer 5′–3′	TTG CAG CTA GGA AGT ACG TCT	21	60.6	
Manf	Forward primer 5′–3′	TCT GGG ACG ATT TTA CCA GGA	21	60.2	PrimerBank ID 142365315c1
	Reverse primer 5′–3′	CTT GCT TCA CGG CAA AAC TTT	21	60.2	

for one week. Following this, OVX mice were injected with HUVEC-Exos or PBS intravenously via the tail vein once weekly for 6 weeks (n = 8 in each group).

Micro-CT experiment

The SkyScan1178 apparatus and related software (Bruker MicroCT, Kontich, Belgium) were used to perform micro-CT scanning and femur analysis. With an energy setting of 35 kV and an intensity of 220 mA, images with a voxel size of 14 microns were acquired. DataViewer and CTVox were used to execute the two- and three-dimensional reconstructions, respectively. As the region of interest (ROI), the trabecular bone at the distal femur's metaphysis under the growth plate was selected. Using CTAn software, the following parameters were found: trabecular number (Tb. N), trabecular thickness (Tb. Th), trabecular separation (Tb. Sp), trabecular bone volume percentage (BV/TV), and bone mineral density (BMD).

TRAP-Staining in vivo

Samples of femur bones from different groups were kept for 24 h in ice-cold 4% paraformaldehyde. For three weeks, bone specimens were decalcified with 10% ethylene diamine tetraacetic acid (EDTA). Following a previous methodology, bone samples were sectioned into 10-μm slices and stained for TRAP [20].

Statistical analysis

GraphPad Prism 8 was used to examine the data, which were then presented as the mean ± standard deviation. It used a one-way analysis of variance or the Student's t-test to assess group data. When the *p*-value was less than 0.05, the data was deemed statistically significant.

Results

Features of HUVEC-Exos

To explore the function of HUVEC-Exos in osteoclast differentiation, TEM, NTA, and WB were performed to identify HUVEC-Exos. HUVEC-Exos showed a distinctive cup-shaped morphology measuring 90–150 nm, as

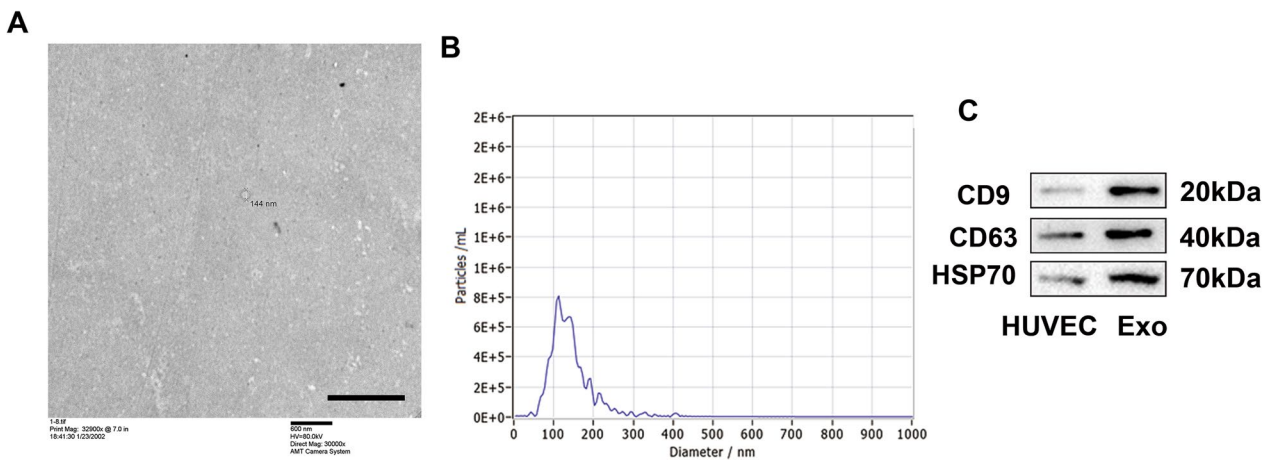

Fig. 1 Characteristics of HUVEC exos. **A** Representative TEM image of HUVEC-Exos (scale bar = 600 nm). **B** Nanoparticle tracking analysis of the size distribution of HUVEC-Exos. **C** HUVEC exos surface markers (CD9, CD63 and HSP70) were detected by WB analysis

shown by TEM and NTA (Fig. 1A, B). The expression of specific protein markers HSP70, CD9, and CD63 in HUVEC-EXos was confirmed by WB analysis (Fig. 1C). The results indicate that the Exos were successfully isolated and purified.

HUVEC-Exos inhibited differentiation of osteoclast in vitro

To investigate the impact on osteoclast differentiation of exosomes produced from HUVEC, The HUVEC-derived exosomes were initially tagged with the Dio, a lipophilic dye. This demonstrated the effective transport of HUVEC-Exos to RAW264.7 cells (Fig. 2A). After that,

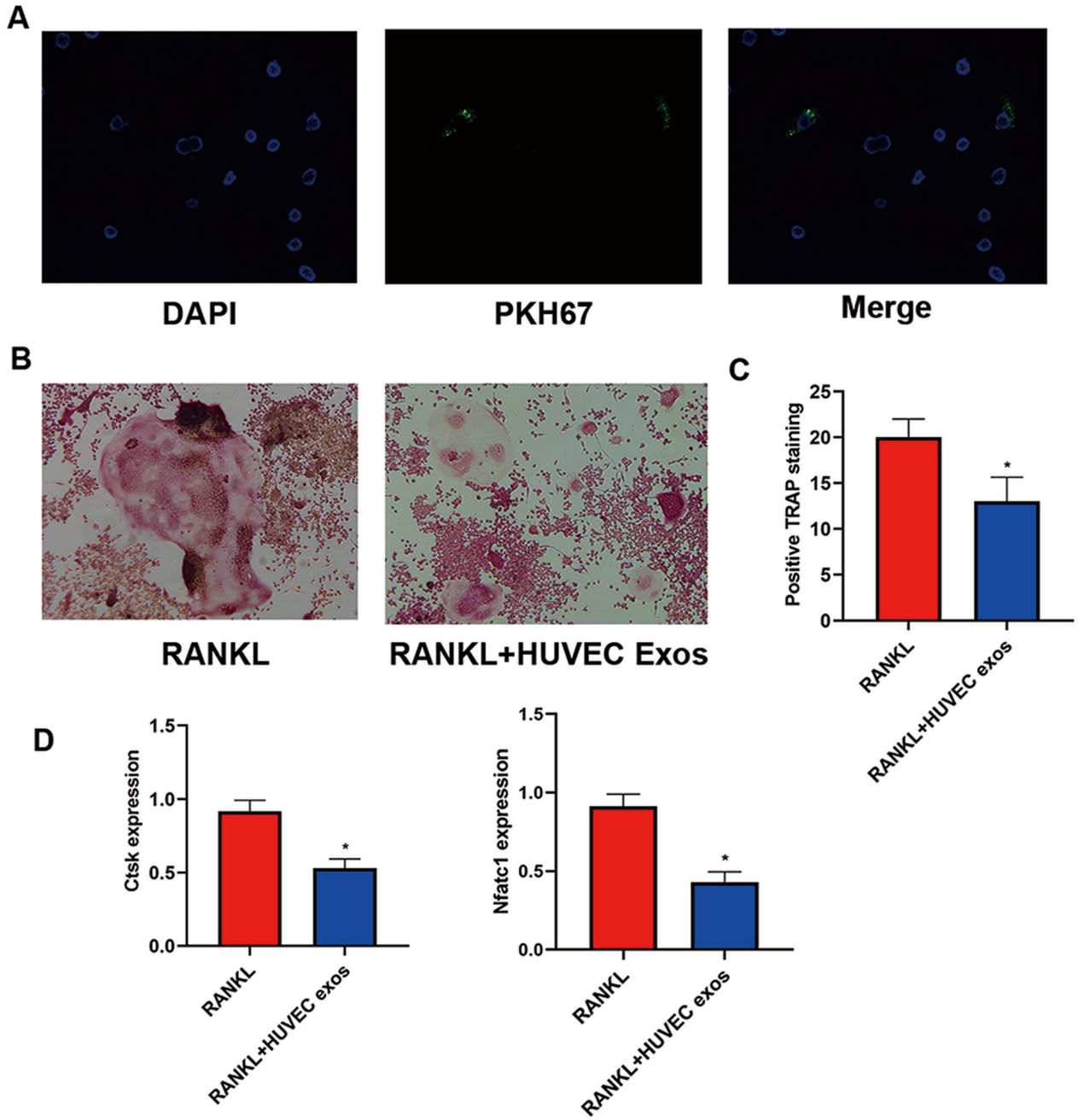

Fig. 2 HUVEC-exos inhibited osteoclast differentiation in vitro. **A** Representative images of PKH67 (green) and DAPI (Blue) immunostaining, scale bar = 100 nm. **B** Representative images of TRAP staining of RAW264.7 cells treated with RANKL or RANKL + HUVEC Exos in vitro, scale bar = 100 nm. **C** quantiative analysis of positive TRAP staining in Fig. 2B (*P < 0.05). **D** Expression levels of Ctsk and Nfatc1 in RAW264.7 cells treated with RANKL or RANKL + HUVEC Exos in vitro (*P < 0.05)

we treated RAW 264.7 cells with PBS or HUVEC-Exos in the same volume. We found that HUVEC-Exos inhibited TRAP staining (Fig. 2B, C). Furthermore, in comparison to the negative control, HUVEC-Exos decreased the expression of Ctsk and Nfatc1. Thus, osteoclast differentiation was inhibited by HUVEC-Exos.

HUVEC-exos target bone in vivo

PKH67-labelled HUVEC-Exos were injected intravenously into 8-week-old male C57BL/6 J mice to investigate whether HUVEC-Exos may target bone in vivo. We evaluated the distribution of PKH67-exosomes by biophotonic imaging at 8 h after injections. The liver exhibited the highest fluorescence signals, whereas detectable signals were seen in the bone tissue (Fig. 3). When combined, HUVEC-Exos may target bone in vivo.

Bone loss was inhibited by HUVEC-exos in vivo

To examine the function of HUVEC-derived exosomes in vivo, an osteoporosis (OP) mice model was generated to confirm whether HUVEC-Exos could relieve bone loss from osteoporosis. Then, we administered HUVEC-Exos or PBS into OVX mice. Micro-CT examination revealed a significant reduction in trabecular separation and increased trabecular bone volume, number, and thickness in OVX mice treated with HUVEC-Exos compared to the PBS group (Fig. 4A, B). Moreover, TRAP staining revealed that the HUVEC-Exos group had a lower osteoclast count than the PBS group (Fig. 4C, D). In a conclusion, HUVEC-Exos could inhibit bone loss in vivo.

HUVEC-exos derived Manf inhibited osteoclast differentiation by targeting NF-κB signaling pathway

To investigate the molecular mechanism through which HUVEC-exos relieve bone loss, we conducted RNA sequencing and statistical analysis of the genes that were differentially expressed. We found that Manf was greater in HUVEC-Exos group than in PBS group (Fig. 5A). Moreover, on day 7, Manf expression was higher in RAW264.7 cells treated with HUVEC-Exos in comparison to the corresponding negative controls (Fig. 5B). Then, to determine the role of Manf in vitro, we treated RAW 264.7 cells with Manf-siRNA or negative control (N.C.). We found that Manf-siRNA promoted TRAP staining in comparsion with its negative control (Fig. 5C, D). Furthermore, Ctsk and Nfatc1expression were increased by Manf-siRNA in comparison with negative control (Fig. 5E).

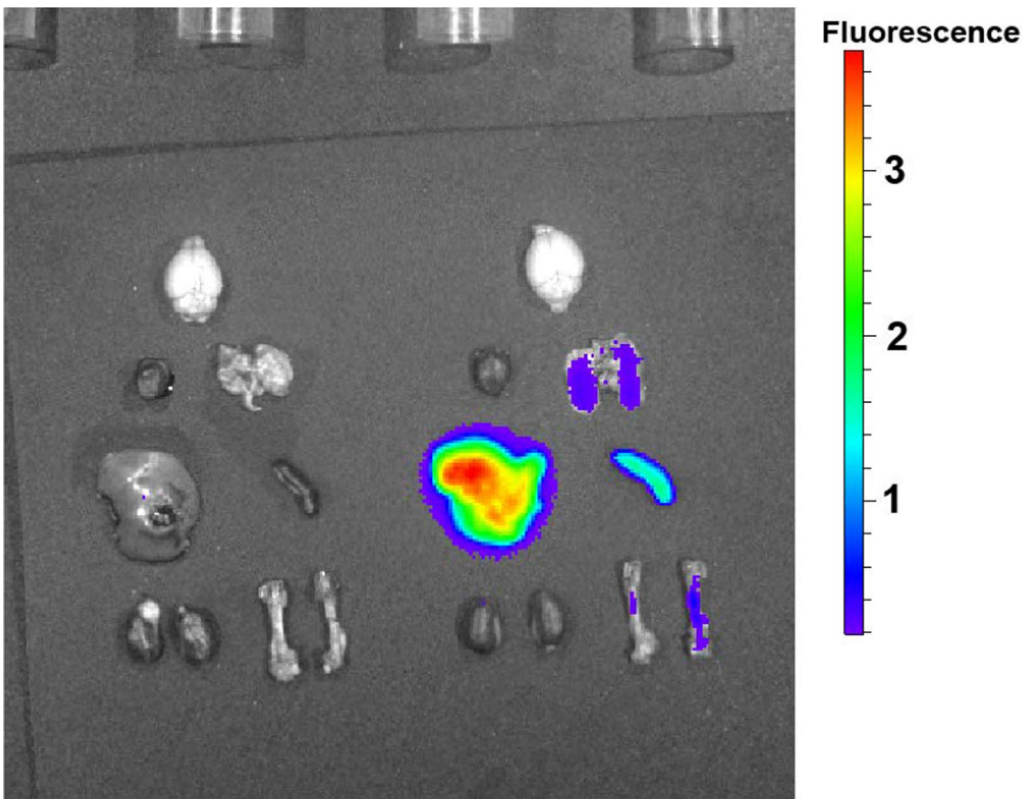

Fig. 3 HUVEC-exos target bone in vivo. Representative images of fluorescence signals in organs harvested from mice treated with PBS or HUVEC exos

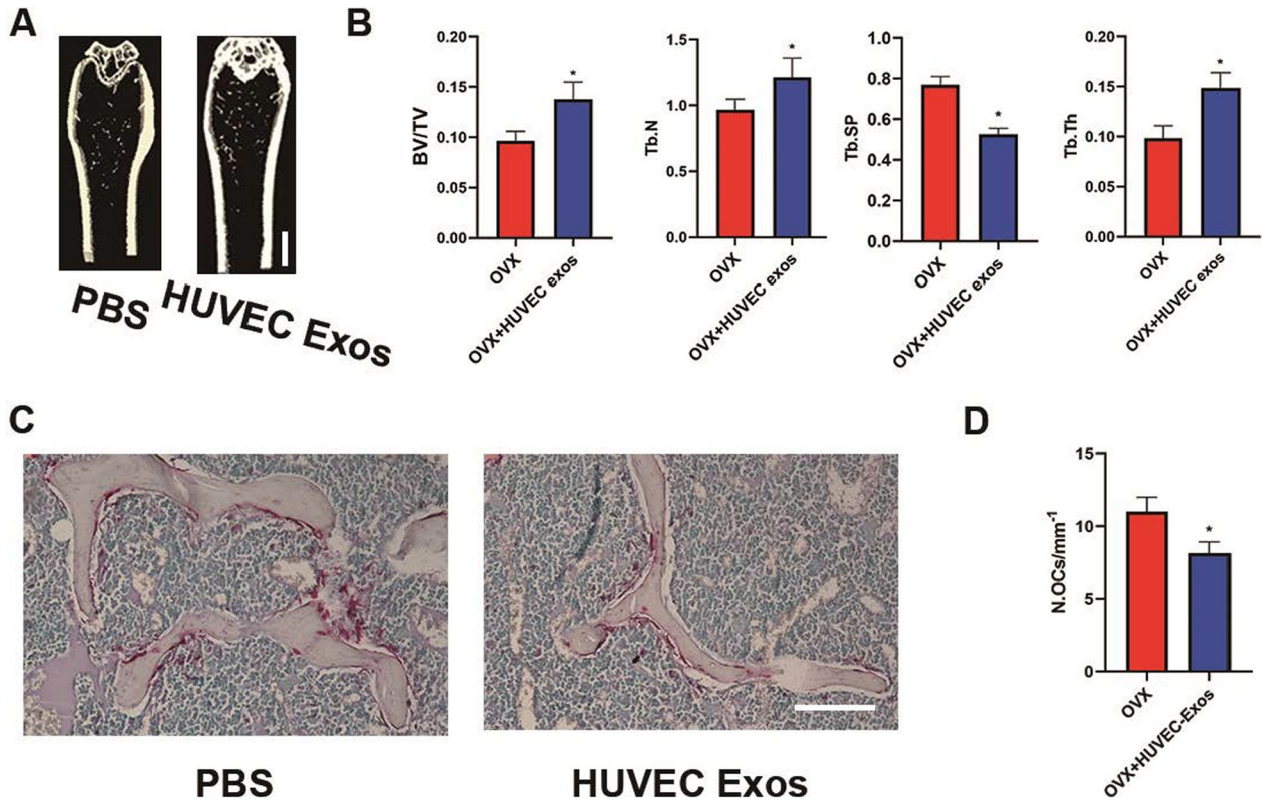

Fig. 4 Bone loss was inhibited by HUVEC-exos in vivo. **A** Representative μCT images of femora from OVX mice treated with PBS or HUVEC exos, scale bar = 300 nm. **B** Quantitative μCT analysis of Fig. 4A. **C** Representative images of TRAP staining in OVX mice femora treated with PBS or HUVEC-Exos, scale bar = 300 nm. **D** Quantitative analysis of the number of osteoclasts (OCs) on trabecular bone surface in Fig. 4C. n = 7 per group

Furthermore, Manf has been reported to fuction through NF-κB pathway. Here, we found that Manf inhibited endogenous levels of P65 protein expression (Fig. 5F, G). Taken together, HUVEC-exosomal Manf inhibited osteoclast differentiation.

HUVEC-exosomal Manf relieved bone loss from osteoporosis

In order to examine Manf's potential as a treatment for osteoporosis, Manf was ultrasonically encapsulated into exosomes generated from HUVEC. The OP mouse model was given HUVEC-exosomal Manf or PBS (negative control) every two weeks for a total of eight weeks. Mice administered HUVEC-exosomal Manf had a significant increase in trabecular bone volume, thickness, and number, along with a decrease in trabecular separation when compared to their negative controls (Fig. 6A, B). Furthermore, P65 expression was lower in femur of OP mice treated with HUVEC-exosomal Manf in comparison to the corresponding negative controls (Fig. 6C). Moreover, TRAP staining revealed that the number of osteoclasts were lower in HUVEC-exosomal Manf group than in negative control group (Fig. 6D, E). Thus, the above data indicates that HUVEC-exosomal Manf suppresses osteoclast differentiation in vivo and alleviates bone loss caused by osteoporosis.

Discussion

By successfully identifying exosomes from HUVEC supernatant cultures, this study showed that exosomes produced from HUVECs may target bone tissue and inhibit the production of osteoclasts in vivo as well as in vitro. Then, We found that HUVEC exosomes upregulate Manf expression in RAW264.7 cells by transcriptome sequencing. Subsequently, we found that Manf inhibited osteoclastgenesis through NF-κB Pathway. Manf was then loaded into HUVEC exosomes. Then, In vivo experiments, HUVEC-Exo^{Manf} rescued bone loss caused by osteoporosis. Our results showed that Manf could be delivered to bone tissue by HUVEC-Exo and was a potential treatment for osteoporosis.

OP is a skeleton disorder, mainly due to metabolic abnormalities, which result in decreased bone mass, changes in bone structure, and reduced bone quality.In the past, it was believed that the Over-activation of osteoclasts causes bone resorption to be greater than bone

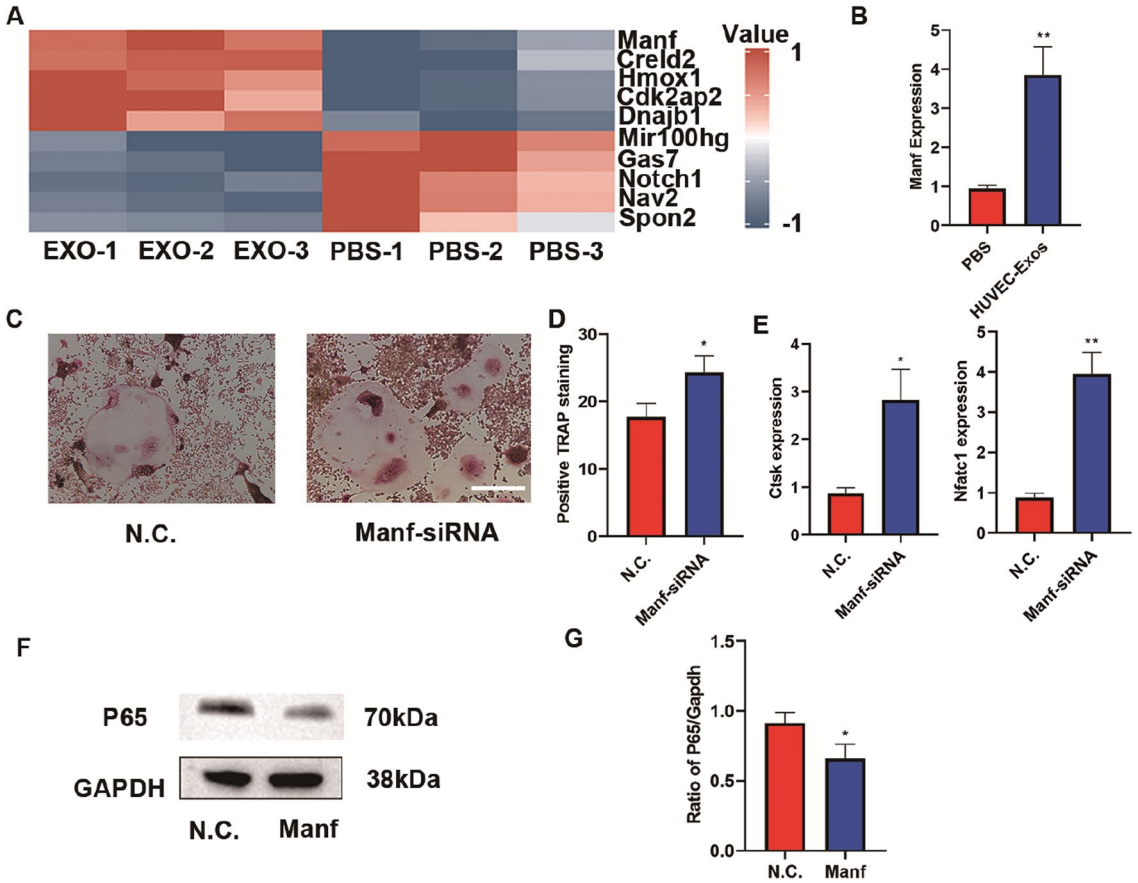

Fig. 5 HUVEC-exos derived Manf inhibited osteoclast differentiation by targeting NF-κB signaling pathway **A** Heatmap of the differentially expressed mRNAs in osteoclasts treated with HUVEC-Exos or PBS group. **B** Expression levels of Manf in RAW264.7 cells treated with RANKL or RANKL + HUVEC Exos in vitro. **C** Representative images of TRAP staining of RAW264.7 cells treated with RANKL + HUVEC Exos or RANKL + HUVEC Exos + Manf-siRNA in vitro, scale bar = 100 nm. **D** quantiative analysis of positive TRAP staining in This figure. **E** Expression levels of Ctsk and Nfatc1 in RAW264.7 cells treated with RANKL + HUVEC Exos or RANKL + HUVEC Exos + Manf-siRNA in vitro **F** Western blot (WB) assay of P65 and GAPDH in RAW 264.7 cells treated with RANKL or RANKL + recombinant Manf **G** quantiative analysis of WB assay in Fig. 5F. (*P < 0.05, **P < 0.01)

formation, resulting in a reduction in bone mass and the eventual development of osteoporosis.

Many studies have supported the role of exosomes as a bone-targeting bionanomaterial. Y. Hu et al. fused CXCR4(+) exosomes with antagomir-188 loaded liposomes to obtain bone-targeting hybrid nanoparticles(NPs) [21]. This nanoparticle enhanced osteogenesis and suppressed adipogenesis in BMSCs, thereby restoring the loss of trabecular bone that occurs with age in vivo. G. Zheng et al. grafted alendronate (ALN) onto polyethylene glycolated phospholipids and subsequently modified PL-derived exosomes(PL-exo) to achieve bone-targeted aggregation [13]. Bone-targeted PL-exo rescued bone loss in osteoporotic mice by promoting osteogenesis and angiogenesis. Furthermore, some exosomes are naturally bone-targeted. Exosomes derived from lung adenocarcinoma cells containing miR-328 could be enriched for bone tissue and promoted osteoclast formation by down-regulating Nrp-2 expression [22]. In a separate study, it was found that vascular endothelial cell-secreted exosomes (EC-Exos) had the ability to target bones and counteract osteoporosis by inhibiting osteoblastic differentiation through miR-155 [17].

Developing targeted drugs is an important part of precision medicine [23]. Exosomes are natural carriers which offer several advantages, including high stability in blood, low immunogenicity, and direct drug delivery to cells [18, 24, 25]. Bone targeting with exosomes often requires surface modifications such as aptamers [26], CXCR4 [21] and alendronate (ALN) modification. However, these modifications can significantly increase the economic cost. In contrast, our delivery of Manf, targeted to bone and using natural exosomes from HUVEC cells, could reduce economic costs.

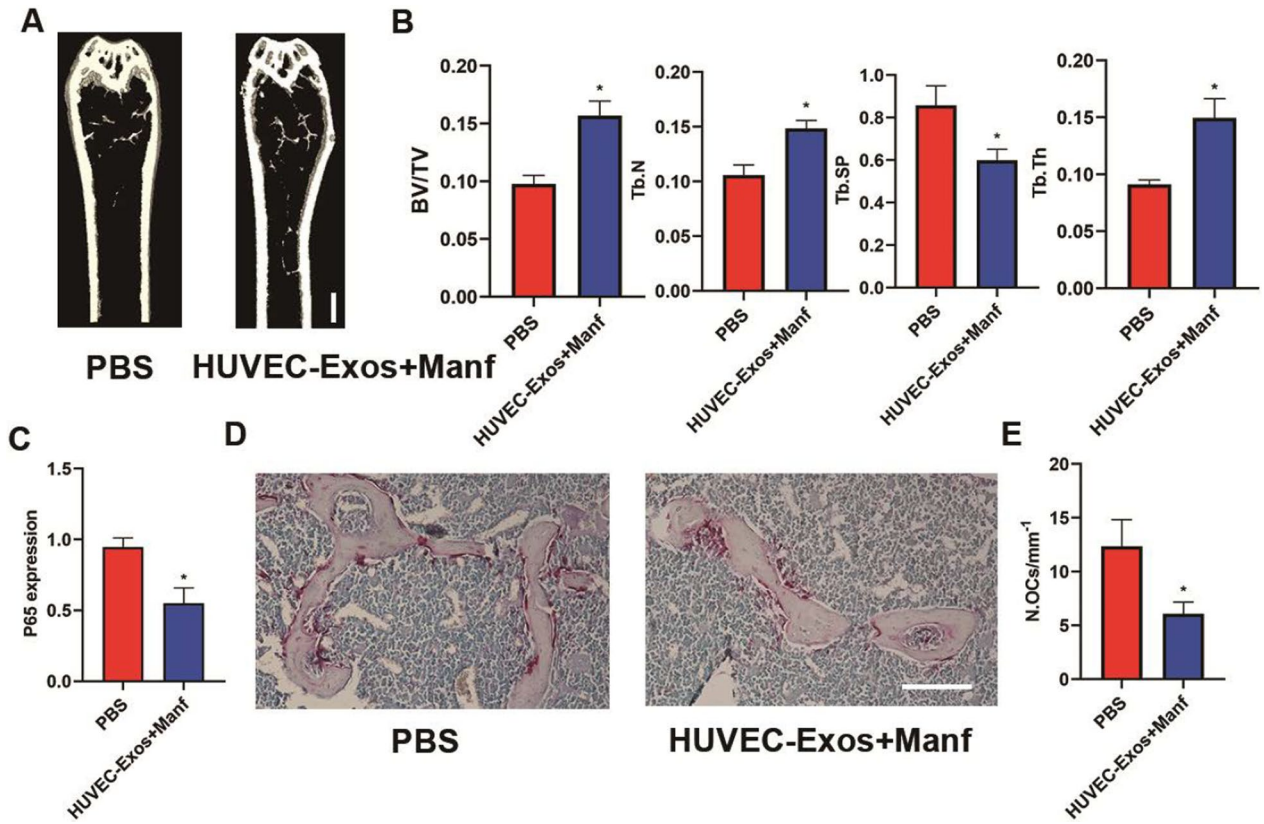

Fig. 6 HUVEC-exosomal Manf relieved bone loss from osteoporosis. **A** Representative μCT images of femora from OVX mice treated with PBS or HUVEC exos^{Manf}, scale bar = 300 nm. **B** Quantitative μCT analysis of Fig. 6A. **C** Expression levels of P65 in the femur of OVX mice treated with PBS or HUVEC exos^{Manf}. **D** Representative images of TRAP staining in OVX mice femora treated with PBS or HUVEC exos.^{Manf}, scale bar = 300 nm. **E** Quantitative analysis of the number of osteoclasts (OCs) on trabecular bone surface in Fig. 6C. n = 7 per group. (*P < 0.05)

Several limitations to the present study should be considered. First, the effectiveness of the results of this study has only been validated in mouse and cellular models. Other animal models must be used for additional validation. Second, the use of exosomes is limited by the difficulty of obtaining large quantities, the high cost of isolating them and the short shelf-life required.

Conclusion

HUVEC-exosomal Manf suppressed osteoclastogenesis via downregulating NF-κB signaling.

Acknowledgements
None.

Author contributions
Zhilong Pi and You Wu. wrote the main manuscript text and, Xinyu Wang prepared Figs. 1–3. Pingyue Li prepared Figs. 4–6. All authors reviewed the manuscript.

Funding
The work is supported by the Guangzhou science and technology project (2024A03J0690).

Availability of data and materials
The datasets generated and/or analysed during the current study are not publicly available due to patient privacy but are available from the corresponding author upon reasonable request. No datasets were generated or analysed during the current study.

Declarations

Ethics approval and consent to participate
This study was approved by the Medical Research Ethics Board of the General Hospital of Southern Theater Command of PLA (No. 20221202), which waived the need for written informed consent due to the retrospective nature of the study. All methods were carried out in accordance with relevant guidelines and regulations.

Consent for publication
Not applicable.

Competing interests
The authors declare that they have no conflicts of interest.

Received: 3 September 2024 Accepted: 3 March 2025
Published online: 07 April 2025

References

1. Gopinath V. Osteoporosis. Med Clin North Am. 2023;107(2):213–25.
2. Eastell R, O'Neill TW, Hofbauer LC, Langdahl B, Reid IR, Gold DT, Cummings SR. Postmenopausal Osteoporosis Nat Rev Dis Primers. 2016;2:16.
3. Johnston CB, Dagar M. Osteoporosis in older adults. Med Clin North Am. 2020;104(5):873–84.
4. Salari N, Ghasemi H, Mohammadi L, Behzadi MH, Rabieenia E, Shohaimi S, Mohammadi M. The global prevalence of osteoporosis in the world: a comprehensive systematic review and meta-analysis. J Orthop Surg Res. 2021;16(1):20.
5. Chen X, Wang ZQ, Duan N, Zhu GY, Schwarz EM, Xie C. Osteoblast-osteoclast interactions. Connect Tissue Res. 2018;59(2):99–107.
6. Boyle WJ, Simonet WS, Lacey DL. Osteoclast differentiation and activation. Nature. 2003;423(6937):337–42.
7. Michiel Pegtel D, Gould SJ. Exosomes. Ann Rev Biochem. 2019;88(1):487–514. https://doi.org/10.1146/annurev-biochem-013118-111902.
8. Colombo M, Raposo G, Théry C. Biogenesis, secretion, and intercellular interactions of exosomes and other extracellular vesicles. Ann Rev Cell Dev Bio. 2014;30(1):255–89. https://doi.org/10.1146/annurev-cellbio-101512-122326.
9. Yin K, Wang SH, Zhao RC. Exosomes from mesenchymal stem/stromal cells: a new therapeutic paradigm. Biomark Res. 2019;7:8.
10. Zhang H, Wang R, Wang G, Zhang B, Wang C, Li D, Ding C, Wei Q, Fan Z, Tang H, et al. Single-cell RNA sequencing reveals B cells are important regulators in fracture healing. Front Endocrinol (Lausanne). 2021;12: 666140.
11. Zhang S, Lu C, Zheng S, Hong G. Hydrogel loaded with bone marrow stromal cell-derived exosomes promotes bone regeneration by inhibiting inflammatory responses and angiogenesis. World J Stem Cells. 2024;16(5):499–511.
12. Li W, Liu Q, Shi J, Xu X, Xu J. The role of TNF-alpha in the fate regulation and functional reprogramming of mesenchymal stem cells in an inflammatory microenvironment. Front Immunol. 2023;14:1074863.
13. Zheng G, Ma H-W, Xiang G-H, He G-L, Cai H-C, Dai Z-H, Chen Y-L, Lin Y, Hua-Zi X, Ni W-F, Cong X, Liu H-X, Wang X-Y. Bone-targeting delivery of platelet lysate exosomes ameliorates glucocorticoid-induced osteoporosis by enhancing bone-vessel coupling. J Nanobiotechnol. 2022. https://doi.org/10.1186/s12951-022-01400-1.
14. Liu X, Shao Y, Tu J, Sun J, Dong B, Wang Z, Zhou J, Chen L, Tao J, Chen J. TMAO-activated hepatocyte-derived exosomes impair angiogenesis via repressing CXCR4. Front Cell Dev Biol. 2021;9: 804049.
15. Gupta A, Cady C, Fauser AM, Rodriguez HC, Mistovich RJ, Potty AGR, Maffulli N. Cell-free stem cell-derived extract formulation for regenerative medicine applications. Int J Mol Sci. 2020;21(24):9364.
16. Gupta A, Shivaji K, Kadam S, Gupta M, Rodriguez HC, Potty AG, El-Amin SF 3rd, Maffulli N. Immunomodulatory extracellular vesicles: an alternative to cell therapy for COVID-19. Expert Opin Biol Ther. 2021;21(12):1551–60.
17. Song H, Li X, Zhao Z, Qian J, Wang Y, Cui J, Weng WZ, Cao LH, Chen X, Hu Y, et al. Reversal of osteoporotic activity by endothelial cell-secreted bone targeting and biocompatible exosomes. Nano Lett. 2019;19(5):3040–8.
18. Zeng WP, Wen ZB, Chen HL, Duan YY. Exosomes as carriers for drug delivery in cancer therapy. Pharm Res. 2023;40(4):873–87.
19. Tian J, Han Z, Song D, Peng Y, Xiong M, Chen Z, Duan S, Zhang L. Engineered exosome for drug delivery: recent development and clinical applications. Int J Nanomed. 2023;18:7923–40.
20. Li B, Wang R, Huang X, Ou Y, Jia Z, Lin S, Zhang Y, Xia H, Chen B. Extracorporeal shock wave therapy promotes osteogenic differentiation in a rabbit osteoporosis model. Front Endocrinol (Lausanne). 2021;12: 627718.
21. Hu Y, Li X, Zhang Q, Gu Z, Luo Y, Guo J, Wang X, Jing Y, Chen X, Su J. Exosome-guided bone targeted delivery of Antagomir-188 as an anabolic therapy for bone loss. Bioact Mater. 2021;6(9):2905–13.
22. Zhang C, Jingru Qin L, Yang ZZ, Yang J, Wan S, Deng H, Wang Z. Exosomal miR-328 originated from pulmonary adenocarcinoma cells enhances osteoclastogenesis via downregulating Nrp-2 expression. Cell Death Discov. 2022. https://doi.org/10.1038/s41420-022-01194-z.
23. Manzari MT, Shamay Y, Kiguchi H, Rosen N, Scaltriti M, Heller DA. Targeted drug delivery strategies for precision medicines. Nat Rev Mater. 2021;6(4):351–70.
24. El Andaloussi S, Maeger I, Breakefield XO, Wood MJA. Extracellular vesicles: biology and emerging therapeutic opportunities. Nat Rev Drug Discov. 2013;12(5):348–58.
25. Kalluri R, LeBleu VS. The biology, function, and biomedical applications of exosomes. Science. 2020;367(6478):640.
26. Luo ZW, Li FX, Liu YW, Rao SS, Yin H, Huang J, Chen CY, Hu Y, Zhang Y, Tan YJ, et al. Aptamer-functionalized exosomes from bone marrow stromal cells target bone to promote bone regeneration. Nanoscale. 2019;11(43):20884–92.

Publisher's Note